

Efficient all-optical helicity-dependent switching in Pt/Co/Pt with dual laser pulses

Kihiro T. Yamada^{1,†,*}, Kiran Horabail Prabhakara^{1,†}, Tian Li², Fuyuki Ando², Sergey Semin¹, Teruo Ono^{2,3}, Andrei Kirilyuk^{1,4}, Alexey V. Kimel^{1,*}, Theo Rasing^{1,*}

¹*Institute for Molecules and Materials, Radboud University Nijmegen, Nijmegen 6525 AJ, The Netherlands*

²*Institute for Chemical Research, Kyoto University, Uji, Kyoto 611-0011, Japan.*

³*Center for Spintronics Research Network (CSRN), Graduate School of Engineering Science, Osaka University*

⁴*FELIX Laboratory, Radboud University Nijmegen, Toernooiveld 7c, 6525 ED Nijmegen, The Netherlands*

[†]These authors contributed equally to this work.

Email*: k.yamada@science.ru.nl; a.kimel@science.ru.nl; th.rasing@science.ru.nl

All-optical helicity-dependent switching (AO-HDS), deterministic control of magnetization by circularly polarized light pulses, allows to efficiently manipulate magnetization without the need of a magnetic field. While ferrimagnetic metals show single-shot magnetization switching, ferromagnetic metals require a large number of pulses to fully reverse the magnetic state from “up” to “down” or vice versa. Here, we demonstrate a drastic reduction in the number of pulses for full switching in a single stack of Pt/Co/Pt. To achieve this, we used pairs of optical pulses, a femtosecond linearly polarized pulse followed by a picosecond circularly polarized pulse. The obtained results suggest that the dual-pulse method is a potential route towards realizing efficient AO-HDS in ferromagnetic metals.

The explosive growth of big data and artificial intelligence demands faster and more energy efficient ways to manipulate and store data¹. One approach is to use current-induced torque to switch magnetization, as in spin-transfer torque magnetic random access memory². Another potential route is to utilize an ultrashort laser pulse³. It was demonstrated that in ferrimagnetic transition metal-rare earth alloys^{4,5}, a single ultrashort laser pulse can switch the magnetization. Furthermore, all-optical helicity-dependent switching (AO-HDS) was recently demonstrated in a variety of ferromagnetic metals, including thin films of Co/Pt⁶⁻¹¹ and Co/Ni⁸, as well as granular alloys with high coercivity, like CoAgPt⁶ and FePt¹². It is now widely accepted that the switching proceeds via two stages: helicity-independent nucleation of switched domains and helicity-dependent deterministic domain wall (DW) motion^{7,9-11}. However, the magnetization reversal from fully “up” to fully “down” requires at least 10^2 - 10^3 light pulses⁶⁻¹².

Here, we demonstrate a dual-pulse method, schematically shown in Fig.1, to realize efficient AO-HDS in a single stack of Pt/Co/Pt with perpendicular magnetic anisotropy. The first short pulse is used to reduce the switching field and the second circularly polarized pulse coming after a constant time separation can efficiently switch the magnetization owing to this reduction. Indeed, we find that 4 pairs of pulses can fully switch the magnetization, when a 90-fs linearly polarized pulse, acting as the first optical pump for demagnetization, and a subsequent 3-ps circularly polarized pulse, as the second optical pump for switching, are used with the pulse interval of 4 ps. In stark contrast, using only circularly polarized pulses, 100 - 150 pulses are still required for fully switching the same stack. Dual-pulse AO-HDS strongly depends on the pulse interval. This unambiguously indicates the ultrafast reduction in the magnetic properties by the first pulse is crucial for the drastic reduction of the pulse number required for switching.

Results

Multi-pulse AO-HDS in the Pt/Co/Pt structure. We used a Pt/Co/Pt stack, which is a typical candidate for spintronic devices² as well as for AO-HDS⁶⁻¹¹. The multilayer of Ta(4 nm)/Pt(3.0 nm)/Co(0.6 nm)/Pt(3.0 nm)/MgO(2.0 nm)/Ta(1 nm) was sputtered on a synthetic quartz glass substrate. DC and RF sources were used for depositing Ta, Pt and Co, and MgO, respectively. The MgO/Ta capping layer prevents the magnetic layer from oxidization. The multilayer exhibits a perpendicular easy axis of magnetization as seen from the perfectly square magnetic hysteresis as a function of perpendicular magnetic field (see Supplementary Information).

In the first set of experiments, we characterized the multi-pulse AO-HDS in the Pt/Co/Pt stack using a static magneto optical set-up (see Methods). Figure 2a shows magneto-optical images taken after the film in down(M^-)/-up(M^+)-magnetized state was excited with 1,000 right(σ^+)/left(σ^-) circularly polarized light pulses, at a repetition rate of 1 kHz. In the experiment, the pulse width τ_σ was varied in the range of 0.5 – 3.0 ps. Uniform AO-HDS is observed for τ_σ in the range of 1.0 – 3.0 ps. However, a slight increase in fluence F_σ results in a multi-domain structure at the spot center. This is due to a larger demagnetized area in comparison to the equilibrium domain size. Figure 2b shows averaged net magnetization $\langle M \rangle$ after illumination with the laser pulses, as a function of τ_σ and F_σ . $\langle M \rangle$ was determined by averaging the intensity of a 15- μm diameter area (within the excited region) and normalizing it to the corresponding intensity when the magnetic state of the same area was fully switched. The $\langle M \rangle$ diagram indicates that a longer pulse width is more suitable for AO-HDS, as already demonstrated by R. Medapalli et al.⁹. In order to better understand the switching process, snapshots were taken before and after pumping the sample with 150 - 800 σ^+ pulses ($\tau_\sigma = 3.0$ ps), as shown in Fig. 2c. It was observed that a few hundred pulses nucleate a switched magnetic domain at the spot center. Subsequent illumination with the pump pulses only increased the switched area by inducing DW motion. Hence, as depicted in Fig.

2d, the switching process can be separated into (i) nucleation of a switched domain and a (ii) subsequent DW propagation.

Dual-pulse AO-HDS in the Pt/Co/Pt structure. In the next set of experiments, we demonstrate that a dual-pulse method is truly much more efficient for AO-HDS. Figure 3a shows snapshots before and after irradiating the sample with 1-5 pair(s) of pulses. Here, the pulse width τ_π and fluence F_π of the linearly polarized pulse were fixed at 90 fs and 2.29 mJ/cm², respectively, corresponding to the demagnetization threshold. The light pulse with circularly polarization ($\tau_\sigma = 3.0$ ps and $F_\sigma = 1.94$ mJ/cm²) was made to reach the sample after a pulse interval $\Delta t = 4.0$ ps. Remarkably, 4 such pulse pairs are sufficient to fully switch the magnetization of a 15- μ m diameter area. This indicates that the dual-pulse method is extremely efficient and a potential approach towards ultrafast AO-HDS in ferromagnetic metals. Dual-pulse AO-HDS with shorter τ_σ is shown in Supplemental Information, which also shows that longer pulses are more suitable for dual AO-HDS than shorter ones. Note that a total of 8 pulses is a record small number amongst the existing reports on AO-HDS in ferromagnetic metals⁶⁻¹², where at least 10^2 - 10^3 light pulses are required for full switching. For comparison, we display the images obtained for multi-pulse excitations with circularly polarized light ($\tau_\sigma = 3.0$ ps and $F_\sigma = 5.48$ mJ/cm²) in Fig. 3b, where the pulse interval between each pulse was set to be at least 1 second. We observed that 100-150 pulses are still required for switching the same area, in contrast to the dual-pulse approach. The required laser fluence increases with decreasing the repetition rate, because the magnetic properties reduce by the accumulated heat in the substrate⁹. The total laser fluence for full switching with the dual-pulse method, $4 \times (F_\pi + F_\sigma) \sim 17$ mJ/cm², is much smaller than $100 \times F_\sigma \sim 548$ mJ/cm² used for the multi-pulse approach. This indicates that the dual-pulse method not only minimizes the number of pulses, but also dramatically reduces the net laser fluence required for switching.

Dual-pulse AO-HDS in the Pt/Co/Pt structure for various pulse interval. To better understand the role of the first short pulse, we varied Δt between the pulses and observed the impact on AO-HDS. Figure 4a shows snapshots taken after illuminating the uniformly magnetized film with 4 dual pulses at positive as well as negative Δt . Here, we used the following laser parameters: $\tau_{\pi} = 90$ fs, $F_{\pi} = 2.35$ mJ/cm², $\tau_{\sigma} = 3.0$ ps, and $F_{\sigma} = 1.26$ mJ/cm². Furthermore, the averaged net magnetization $\langle M \rangle$ after 4 pairs of pulses is plotted in Fig. 4b as a function of Δt . $\langle M \rangle$ was determined in the same manner as in the previous section. When the circularly polarized pulse reaches the film before the linearly polarized pulse ($\Delta t < 0.0$ ps), a multi-domain state is stabilized ($\langle M \rangle \sim 0.0$) because the linearly polarized pulse has demagnetized the magnetic state. When the two pulses simultaneously arrive at the film ($\Delta t = 0.0$ ps), the multi-domain area is maximized. With increasing Δt beyond 0.0 ps, the multi-domain area shrinks and a uniformly switched area appears near the outmost DW; eventually, the multi-domain area disappears and $\langle M \rangle$ gets to -1.0 at around $\Delta t = 4.0$ ps. A further increase in Δt drastically decreases the switched area and increases $\langle M \rangle$. These observations indicate that the ultrafast reduction of the magnetic properties triggered by the first short pulse and the pulse interval and order of the two pulses are crucial for dual-pulse AO-HDS.

Discussion

The first important question is: what is the driving force behind AO-HDS in ferromagnetic metals? The obtained results show a clear light helicity dependence of the switching process. This means that the circularly polarized light breaks the degeneracy between two domains with opposite magnetization orientations. Therefore, the effect of the pulse can be expressed in forms of an effective magnetic field. Quantum mechanical treatment of the inverse Faraday effect¹³ showed that, next to a relatively small magnetic polarization, a light pulse induces an effective

Zeeman field. The peak amplitude of the effective Zeeman field is proportional to the square of the laser electric field in the system ; for instance, stretching the pulse width from 90 fs to 3.0 ps reduces the peak amplitude to 3.0 % at a constant fluence. Since the life time of the photo-excited electrons in Co is short (less than 2 fs at 1.55 eV¹⁴) with respect to the pulse duration, an increase in pulse duration will significantly decrease the strength of this opto-magnetic phenomenon. Therefore, the inverse Faraday effect is an unlikely candidate to explain the result that the longer pulse is more suitable for AO-HDS in the present system.

Magnetic circularly dichroism (MCD) can produce a heat gradient across a DW, and subsequently push a DW from the hotter (lower DW energy) to the colder (higher DW energy) area⁷⁻¹¹, as the up (down)-magnetized domain absorbs the left (right) circularly polarized light more than the down (up)- magnetized domain. During the cooling process, the DW does not move back to the initial position due to pinning. When a circularly polarized pulse with $F_{\sigma} = 5.48 \text{ mJ/cm}^2$ illuminates the Pt/Co/Pt stack, the heat gradient across a DW is estimated to be $\nabla T = (\Delta A_{\text{MCD}} F_{\sigma}^*) / [w_{\text{DW}} C (t_{\text{Co}} + t_{\text{Pt}})] = 1.7 \text{ K/nm}$. Here, we used an absorbed fluence F_{σ}^* of 2.20 mJ/cm^2 , a typical DW width $w_{\text{DW}} = 10 \text{ nm}$, an MCD coefficient⁸ $\Delta A_{\text{MCD}} = 0.015$, a weighted heat capacity¹⁵ $C = 2.93 \text{ MJ/Km}^3$, a Co thickness $t_{\text{Co}} = 0.6 \text{ nm}$, and a Pt thickness $t_{\text{Pt}} = 6.0 \text{ nm}$, respectively. F_{σ}^* was calculated using the complex refractive indices¹⁵ of Co ($2.97 + 4.87i$) and Pt ($2.84 + 4.96i$) at the wavelength of 800 nm and the thickness values given above. The heat gradient across a DW produced by the illumination of the circularly polarized pulse is five orders of magnitude larger than when using a conventional way¹⁶ with heaters to produce a lateral heat gradient. This giant heat gradient can generate large spin transfer torques¹⁷⁻¹⁹ to a DW and move it. Note that it is clear that the temperature gradient increases with increasing the total energy of the laser pulse, apart from the relevant mechanisms. Therefore, the longer pulse can supply larger energy to the

system without demagnetizing²⁰ and thus should be more suitable for AO-HDS under this scenario.

The second important question to discuss now is: why is the dual-pulse method more efficient than the multi-pulse method? Ultrafast demagnetization triggered by the first pulse is crucial to explain this. Just after the arrival of the first short pulse, the magnetization drastically decreases on a time scale of hundreds of femtoseconds (see ref. ²⁰⁻²⁴ and Supplementary Information). When the fluence of the short pulse reaches the critical level at which the electron temperature reaches the Curie temperature (T_C), a paramagnetic-like state appears^{23,24} (Fig. 5a). A switched domain is indeed observed at the center of the spot when using only the short linearly polarized pulse at the demagnetization threshold (see Supplementary Information). Therefore, the fluence of the first pulse was high enough to create the paramagnetic-like states around the center of the spot. After the paramagnetic-like state, small switched domains nucleate stochastically. Subsequently, each domain absorbs an amount of energy from the subsequent long pulse depending on the magnetic orientations and the light helicity. The thus formed heat gradients across the DWs move them. The cooler domains expand and merge to form larger domains, whereas the hotter domains shrink to disappear. We note that there should be an optimal pulse interval between the two pulses in the dual-pulse switching processes, as observed in Fig. 4. When the pulse interval is too short, the domains return to the paramagnetic-like state because the spin temperature rises again to T_C . On the other hand, when the pulse interval is too long, the recovered magnetic properties can slow down the DW motion. Therefore, to move the DW efficiently, the spin temperature should be as close to T_C as possible but must stay below T_C .

In the case of the single-pulse excitation, the laser pulse has almost passed through the system before the magnetization reaches the minimum²⁰ and switched domains nucleate. Understandably, a heat gradient across a DW never forms unless a switched domain already exists. Even when switched domains already exist, the single-pulse excitation is inefficient

because the reduction of the magnetization and the formation of the heat gradient across a DW develop simultaneously.

In conclusion, we have demonstrated that our dual-pulse method can drastically reduce the pulse number required for AO-HDS in a Pt/Co/Pt structure. Using a linearly polarized femtosecond pulse for the first pump and a circularly polarized picosecond pulse for the second pump, we successfully realized a record small number of 8 pulses to fully switch a magnetic domain. In the dual-pulse method, the pulse interval between the different functional pulses is important. This means that the ultrafast decrease in the magnetic properties triggered by the first pulse is crucial for reducing the number of pulses for deterministic AO-HDS. This research suggests that the dual-pulse method is a potential route towards realizing efficient AO-HDS in ferromagnetic metals.

Methods

Optical measurement set-up for imaging. For optical excitation we used a Ti:sapphire amplified laser system (Solstice Ace, Spectra-Physics) of which the central wavelength and repetition rate were 800 nm and 1 KHz, respectively. The amplifier system contains two compressors which allowed independent control of pulse width for two pump beam beams. The laser amplifier was used in external trigger mode, in which with the help of delay generator (DG645, Stanford Research) we can control the amount of pulses reaching the sample. To detect the magnetic state, magneto-optical Faraday imaging with a white light as probe was employed as depicted in Fig. S1 in the Supplementary Information. The first linearly polarized pump pulse had a width, τ_{π} , of 90 fs while the second, circularly polarized pump pulse, had a variable width, τ_{σ} , in the range of 0.5 – 3.0 ps and arrived after an adjustable time interval, Δt . The laser pulses had a Gaussian intensity distribution and both were incident at an angle of 15 deg. from the sample normal. The focused beam sizes ($1/e^2$ radius) for the pump pulses were calculated based on the Liu-method

²⁵ (see Supplemental Note 3). The laser fluence was calculated using the $1/e^2$ radius, the repetition rate (1 kHz), and the average power measured with a power meter. The pump intensity was controlled using a combination of a half wave plate and a Gran-Taylor prism. To achieve precise intensity control of the circularly-polarized pump, the half wave plate was mounted on a motorized stage. A quarter wave plate was placed after the Gran-Taylor prism to convert the linearly polarized beam to a circularly polarized one for the second pump. The probe light from the white light source was linearly polarized by a sheet polarizer. It was then collimated and incident on the sample surface using a combination of lenses. The transmitted light from the sample was collected by an objective with a magnification of 20x. An analyzer, with the polarization axis orthogonal to the polarization of the incident probe light, was placed before a charge-coupled device camera.

References

1. Manipatruni, S., Nikonov, D. E. & Young, I. A. Beyond CMOS computing with spin and polarization. *Nat. Phys.* **14**, 338-343 (2018).
2. Brataas, A., Kent, A. D., & Ohno, H. Current-induced torques in magnetic materials. *Nat. Mater.* **11**, 372-381 (2012).
3. Kirilyuk, A., Kimel, A. V. & Rasing Th. Ultrafast optical manipulation of magnetic order. *Rev. Mod. Phys.* **82**, 2731-2784 (2010).
4. Stanciu, C. D., Hansteen, F., Kimel, A. V., Kirilyuk, A., Tsukamoto, A., Itoh, A. & Rasing Th. All-optical magnetic recording with circularly polarized light. *Phys. Rev. Lett.* **99**, 047601 (2007).

5. Ostler, T. A., Barker, J., Evans, R. F. L., Chantrell, R. W., Atxitia, U., Chubykalo-Fesenko, O., Moussaoui, S. El, Guyader, L. Le, Mengotti, E., Heyderman, L. J., Nolting, F., Tsukamoto, A., Itoh, A., Afanasiev, D., Ivanov, B. A., Kalashnikova, A. M., Vahaplar, K., Mentink, J., Kirilyuk, A., Rasing, Th. & Kimel, A.V. Ultrafast heating as a sufficient stimulus for magnetization reversal in a ferrimagnet. *Nat. Commun.* **3**, 666 (2012).
6. Lambert, C-H., Mangin, S., Varaprasad, B. S. D. Ch. S., Takahashi, Y. K., Hehn, M., Cinchetti, M., Malinowski, G., Hono, K., Fainman, Y., Aeschlimann, M. & Fullerton, E. E. All-optical control of ferromagnetic thin films and nanostructures. *Science* **345**, 1337-1340 (2014).
7. Hadri, M. S. El, Pirro, P., Lambert, C.-H., Petit-Watelot, S., Quessab, Y., Hehn, M., Montaigne, F., Malinowski, G. & Mangin, S. Two types of all-optical magnetization switching mechanisms using femtosecond laser pulses. *Phys. Rev. B* **94**, 064412 (2016).
8. Hadri, M. S. El, Hehn, M., Pirro, P., Lambert, C.-H., Malinowski, G., Fullerton, E. E. & Mangin, S. Domain size criterion for the observation of all-optical helicity-dependent switching in magnetic thin films. *Phys. Rev. B* **94**, 064419 (2016).
9. Medapalli, R., Afanasiev, D., Kim, D. K., Quessab, Y., Manna, S., Montoya, S. A., Kirilyuk, A., Rasing, Th., Kimel, A. V. & Fullerton, E. E. Multiscale dynamics of helicity-dependent all-optical magnetization reversal in ferromagnetic Co/Pt multilayers. *Phys. Rev. B* **96**, 224421 (2017).
10. Quessab, Y., Medapalli, R., Hadri, M. S. El, Hehn, M., Malinowski, G., Fullerton, E. E. & Mangin, S. Helicity-dependent all-optical domain wall motion in ferromagnetic thin films. *Phys. Rev. B* **97**, 054419 (2018).
11. Parlak, U., Adam, R., Bürgler, D. E., Gang, S. & Schneider, C. M. Optically induced magnetization reversal in [Co/Pt]_N multilayers: Role of domain wall dynamics. *Phys. Rev. B* **98**, 214443 (2018).

12. John, R., Berritta, M., Hinzke, D., Müller, C., Santos, T., Ulrichs, H., Nieves, P., Walowski, J., Mondal, R., Chubykalo-Fesenko, O., McCord, J., Oppeneer, P. M., Nowak, U. & Münzenberg, M. Magnetisation switching of FePt nanoparticle recording medium by femtosecond laser pulses. *Sci. Rep.* **7**, 4114 (2017).
13. Berritta, M., Mondal, R., Carva, K. & Oppeneer, P. M. *Ab Initio* theory of coherent laser-induced magnetization in metals. *Phys. Rev. Lett.* **117**, 137203 (2016).
14. Knorren, R., Bennemann, K. H., Burgermeister, R. & Aeschlimann, M. Dynamics of excited electrons in copper and ferromagnetic transition metals: Theory and experiment. *Phys. Rev. B* **61**, 9427 (2000).
15. Rumble, J. R. (ed.) CRC Handbook of Chemistry and Physics, 99th edn (CRC Press, Boca Raton, 2017).
16. Uchida, K., Ota, T., Harii, K., Takahashi, S., Maekawa, S., Fujikawa, Y. & Saitoh, E. Spin-Seebeck effects in $\text{Ni}_{81}\text{Fe}_{19}/\text{Pt}$ films. *Solid State Commun.* **150**, 524 (2010).
17. Hatami, M., Bauer, G. E. W., Zhang, Q. & Kelly, P. J. Thermal spin-transfer torque in magnetoelectronic devices. *Phys. Rev. Lett.* **99**, 066603 (2007).
18. Yu, H., Granville, S., Yu, D. P. & Ansermet, J.-Ph. Evidence for thermal spin-transfer torque. *Phys. Rev. Lett.* **104**, 146601 (2010).
19. Hinzke, D. & Nowak, U. Domain Wall Motion by the Magnonic spin Seebeck effect. *Phys. Rev. Lett.* **107**, 027205 (2011).
20. Fognini, A., Salvatella, G., Gort, R., Michlmayr, T., Vaterlaus, A. & Acremann, Y. The influence of the excitation pulse length on ultrafast magnetization dynamics in nickel. *Struct. Dyn.* **2**, 024501 (2015).
21. Beaurepaire, E., Merle, J.-C., Daunois, A. & Bigot, J.-Y. Ultrafast spin dynamics in ferromagnetic nickel. *Phys. Rev. Lett.* **76**, 4250-4253 (1996).

22. Koopmans, B., Malinowski, G., Dalla Longa, F., Steiauf, D., Föhnle, M., Roth, T., Cinchetti, M. & Aeschlimann, M. Explaining the paradoxical diversity of ultrafast laser-induced demagnetization. *Nat. Mater.* **9** 259-265 (2010).
23. Tengdin, P., You, W., Chen, C., Shi, X., Zusin, D., Zhang, Y., Gentry, C., Blonsky, A., Keller, M., Oppeneer, P. M., Kapteyn, H. C., Tao, Z. & Murnane, M. M. Critical behavior within 20 fs drives the out-of-equilibrium laser-induced magnetic phase transition in nickel. *Sci. Adv.* **4**, 977 (2018).
24. You, W., Tengdin, P., Chen, C., Shi, X., Zusin, D., Zhang, Y., Gentry, C., Blonsky, A., Keller, M., Oppeneer, P. M., Kapteyn, H., Tao, Z. & Murnane, M. Revealing the nature of the ultrafast magnetic phase transition in Ni by correlating extreme ultraviolet magneto-optic and photoemission spectroscopies. *Phys. Rev. Lett.* **121**, 077204 (2018).
25. Liu, J. M. Simple technique for measurements of pulsed Gaussian-beam spot sizes. *Opt. Lett.* **7**, 196-198 (1982).

Acknowledgements

We thank T. Toonen and C. Berkhout for the continuous technical supports. We also appreciate T. Taniguchi for the valuable comments on sample fabrication. This work was partly supported by the European Research Council Grant Agreement No. 339813 (Exchange), the FOM programme Exciting Exchange, de Nederlandse Organisatie voor Wetenschappelijk Onderzoek (NWO), the EU H2020 Program Grant Agreement No. 713481 (SPICE), spintronic-photonic integrated circuit platform for novel electronics, and Grants-in-Aid for Specially Promoted Research from JSPS No. 15H05702.

Author contributions

K.T.Y, A.V.K, and T.R. conceived the experiments. K.T.Y., K.H.P., and S.S. designed and build the experimental set-up. K.T.Y. and K.H.P performed the measurements, and collected data. All the data were analyzed by K.T.Y. and K.H.P with the help of A.K., A.V. K and T.R. The samples were fabricated and provided by T.L., A.F., and T.O. K.T.Y., K.H.P, A.V.K., and T.R. wrote the manuscript. All authors discussed the results and commented on the manuscript. This project was coordinated by A.V.K. and T. R.

Additional information

Supplementary information is available in the online version of the paper. Reprints and permissions information is available online at www.nature.com/reprints. Correspondence and request for materials should be addressed to K.T.Y., A.V.K, and T.R.

Competing financial interests

The authors declare no competing financial interests.

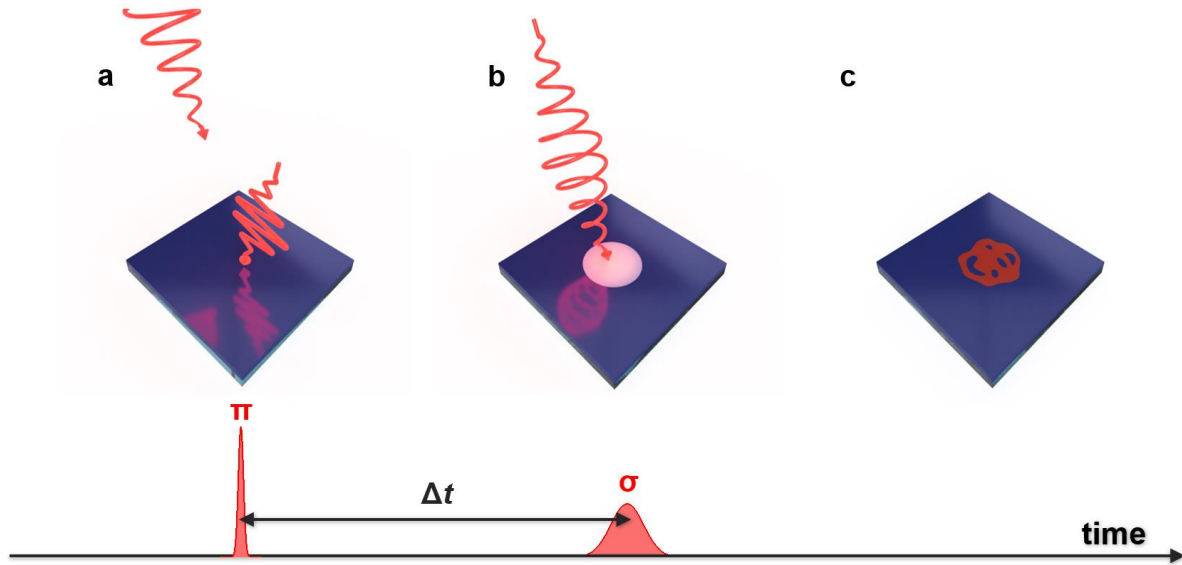


Fig. 1 Principal concept of dual-pulse all-optical helicity-dependent switching (AO-HDS). **a-c** Schematic figures of switching process by dual-pulse excitation in a perpendicularly magnetized film. A short linearly polarized (π) pulse arrives at the down-magnetized system (**a**) and decreases the magnetic properties, resulting in reduction in the energy barrier for the magnetization switching. The longer circularly polarized (σ) pulse reaches the film after a constant pulse interval (Δt) (**b**), and induces a helicity-dependent effective magnetic field to switch the magnetization. In this case, an up-magnetized state is anticipated as the final state, as depicted in (**c**).

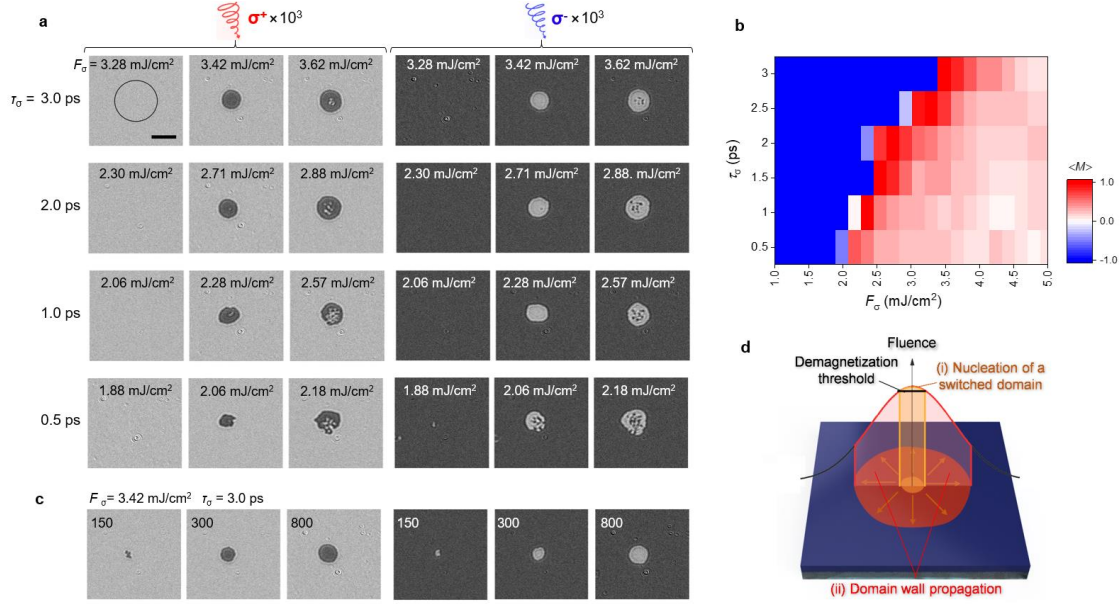


Fig. 2 Pulse width dependence (τ_p) of AO-HDS with multiple pulses. **a** AO-HDS by multiple pulses of circularly polarized laser with τ_p in the range of 0.5 -3.0ps. Each magneto-optical image was taken after illuminating the uniformly magnetized film with 1,000 pulses of right (σ^+) or left (σ^-) circular polarization with a constant fluence (F_0) at a laser repetition rate of 1 kHz. The darker (brighter) area denotes up (down)-magnetization. A continuous-line circle indicates the size of the focused circularly polarized pulse (52.0 ± 0.8 μm in diameter). The scale bar corresponds to 30 μm . **b** Averaged net magnetization $\langle M \rangle$ after 1,000 circularly polarized pulses plotted as function of τ_p and F_0 . $\langle M \rangle = -1$ means that the magnetic state of a 15- μm diameter area is the same as the initial one, and $\langle M \rangle$ reaches 1 when the magnetization is uniformly switched. **c** Magneto-optical images after illumination with 150, 300, and 800 circularly polarized pulses. Here, the value of F_0 was fixed at 3.42 mJ/m². **d** Schematic illustration of the switching process of multi-pulse AO-HDS. When the central fluence of the Gaussian laser spot goes above the demagnetization threshold, a switched domain nucleates at the spot center. Then, the domain wall concentrically propagates driven by circularly polarized pulses.

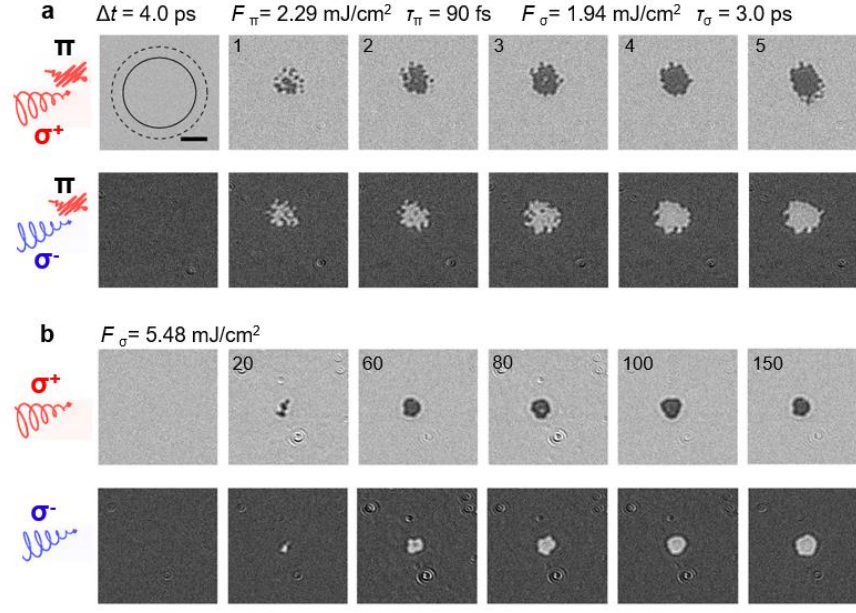


Fig. 3 AO-HDS with dual pulses. **a** Magneto-optical images after dual-pulse excitations. We used a 90-fs linearly polarized laser pulse with fluence (F_{π}) of 2.29 mJ/cm² as the first pump pulse. A 3-ps circularly polarized pulse with fluence (F_{σ}) of 1.94 mJ/cm² reaches the sample after a pulse interval (Δt) of 4.0 ps. **b** Magneto-optical images obtained under multi-pulse excitation for comparison. The images were taken after illumination with circularly polarized pulses with $F_{\sigma} = 1.94$ mJ/cm², where the pulse interval was set to be at least 1 second to compare the two cases. The numbers of (pairs of) pulses are shown in the snapshots. The sizes of the circularly and linearly polarized pulses are indicated by continuous- and broken-line circles, 68.2 ± 1.8 and 52.0 ± 0.8 μ m in diameter, respectively. The scale bar corresponds to 20 μ m.

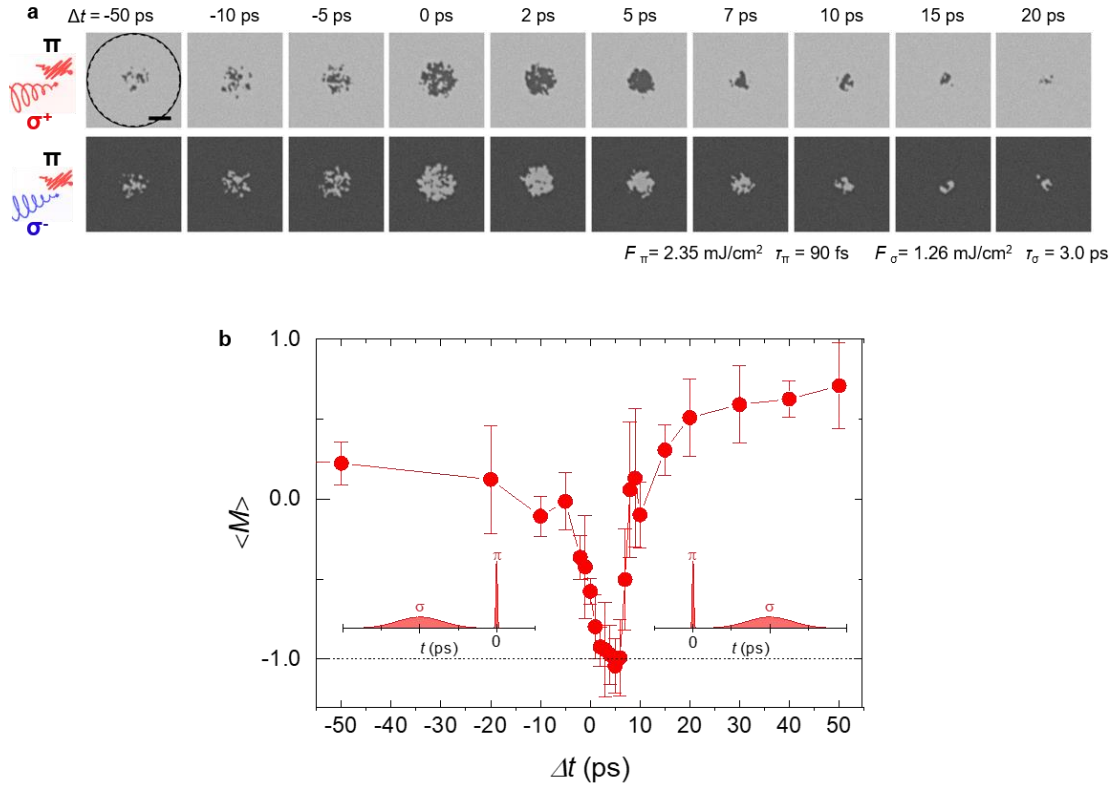


Fig. 4 Pulse interval (Δt) dependence of dual-pulse AO-HDS. **a** Snapshots after 4 pairs of pulses at positive and negative Δt . Here, we used a 90-fs linearly polarized laser pulse with fluence (F_π) of 2.29 mJ/cm² and 3.0-ps circularly polarized laser pulse with fluence (F_σ) of 2.29 mJ/cm². Positive (Negative) Δt means that the linearly polarized pulse arrives at the film earlier (later) than the circularly polarized pulse. The spot sizes of the circularly (continuous-line circle) and linearly polarized (broken-line circle) pulses are 84.2 ± 1.2 and 82.7 ± 1.0 μm in diameter, respectively. The scale bar corresponds to 20 μm . **b** Averaged net magnetization $\langle M \rangle$ after 4 pairs of pulses as a function of Δt . $\langle M \rangle = -1$, 0, and +1 correspond to initial uniformly-magnetized, demagnetized, and fully-switched states of a 15- μm diameter area, respectively.